Bioscience Reports (2019) **133** 1053–1066
https://doi.org/10.1042/CS20190110

PORTLAND PRESS

Research Article

CircRASSF2 promotes laryngeal squamous cell carcinoma progression by regulating the miR-302b-3p/IGF-1R axis

Linli Tian, Jing Cao, Hui Jiao, Jiarui Zhang, Xiuxia Ren, Xinyu Liu, Ming Liu and Yanan Sun

Department of Otorhinolaryngology, Head and Neck Surgery, The Second Affiliated Hospital, Harbin Medical University, No. 148 Baojian Road, Nangang District, Harbin 150086, China

Correspondence: Ming Liu (jianguang1612@163.com) and Yanan Sun (76202920@qq.com)

Background: Circular RNAs (circRNAs) are a class of non-coding RNAs (ncRNAs) broadly expressed in cells of various species. However, the molecular mechanisms that link circRNAs with laryngeal squamous cell carcinoma (LSCC) are not well understood. In the present study, we attempted to provide novel basis for targeted therapy for LSCC from the aspect of circRNA–microRNA (miRNA)–mRNA interaction.
Methods: We investigated the expression of circRNAs in three paired LSCC tissues and adjacent non-tumor tissues by microarray analysis. Differentially expressed circRNAs were identified between LSCC tissues and non-cancerous matched tissues, including 527 up-regulated circRNAs and 414 down-regulated circRNAs. We focused on hsa_circ_0059354, which is located on chromosome 20 and derived from RASSF2, and thus we named it circRASSF2.
Results: circRASSF2 was found to be significantly up-regulated in LSCC tissues and LSCC cell lines compared with paired adjacent non-tumorous tissues and normal cells. Moreover, knockdown of circRASSF2 significantly inhibited cell proliferation and migration *in vitro*, which was blocked by miR-302b-3p inhibitor. Bioinformatics analysis predicted that there is a circRASSF2/miR-302b-3p/ insulin-like growth factor 1 receptor (IGF-1R) axis in LSCC progression. Dual-luciferase reporter system validated the direct interaction of circRASSF2, miR-302b-3p, and IGF-1R. Western blot verified that inhibition of circRASSF2 decreased IGF-1R expression. Furthermore, silencing circRASSF2 suppressed LSCC growth *in vivo*. Importantly, we demonstrated that circRASSF2 was up-regulated in serum exosomes from LSCC patients. Altogether, silencing circRASSF2 suppresses progression of LSCC by interacting with miR-302b-3p and decreasing inhibiting IGF-1R expression.
Conclusion: In conclusion, these data suggest that circRASSF2 is a central component linking circRNAs to progression of LSCC via an miR-302b-3p/IGF-1R axis.

Introduction

Laryngeal squamous cell carcinoma (LSCC) is a common malignancy of the head and neck [1]. The current standard treatment for LSCC including debulking surgery, radiation therapy, and chemotherapy have a moderate effect on early-stage cases; however, the overall 5-year survival rate for patients with advanced LSCC remains poor [2,3]. The high invasiveness and acquired resistance to chemotherapy lead to severe recurrence of LSCC [4]. Hence, it is significant to unveil underlying mechanism of LSCC progression and pathogenesis.

Circular RNAs (circRNAs) are recently identified as members of the non-coding RNA (ncRNAs) family that play a significant role in many cancers progression [5,6]. Numerous studies have reported that

Received: 27 February 2019
Revised: 08 April 2019
Accepted: 15 April 2019

Accepted Manuscript Online: 16 April 2019
Version of Record published: 09 May 2019

Bioscience Reports (2019) **133** 1053–1066
https://doi.org/10.1042/CS20190110

abnormal expressions of circRNAs are closely related to malignant behaviors of various tumors, including LSCC [7,8]. Fan et al. [9] identified 506 differentially expressed circRNAs from human LSCC and normal laryngeal mucosa tissues, and functional analysis revealed that circ-0044520 and circ-0044529 play important regulatory roles by sponging miR-4726-5p and miR-4640-5p.

Exosomes are small membrane-derived vesicles with a diameter of approximately 30–150 nm [10]. They play crucial role in tumor proliferation and metastasis as mediators of cell-to-cell communication by transferring and exchanging oncogenic molecules, which includes lncRNAs and circRNAs [11,12]. Additionally, exosomal circRNAs as clinical biomarkers are stable in blood and could be promising novel biomarkers used for the clinical detection [13]. However, the roles and functions of exosomal circRNAs from LSCC cells still remain largely uncovered.

Here, using a circRNA microarray profiling, we report that the expression of circRASSF2 is markedly elevated both in LSCC tissues and exosomes from LSCC plasma. By modulating miR-302b-3p/insulin-like growth factor 1 receptor (IGF-1R) axis, circRASSF2 enhances the proliferation, migration, and invasion of LSCC cells. Our findings will provide new insights into the regulatory mechanisms of circRASSF2 in LSCC progression.

Methods

The Cancer Genome Atlas dataset analysis

The data and the corresponding clinical information of patients were collected from the Cancer Genome Atlas (TCGA) database (http://cancergenome.nih.gov/). We used the edgeR package of R packages to perform the difference analysis (http://www.bioconductor.org/packages/release/bioc/html/edgeR.html) and used the pheatmap package of R packages to perform the cluster analysis (https://cran.r-project.org/web/packages/pheatmap/index.html). Sva R package was used to remove the batch effect. Genes with adjusted P-values <0.05 and absolute fold changes (FC) > 1.5 were considered differentially expressed genes. Kaplan–Meier survival curves were drawn to analyze the relationships between genes and overall survival in the survival package. The corresponding statistical analysis and graphics were performed in R software (R version 3.3.2).

Tissue samples

A total of 85 pairs of tumor tissue and adjacent normal tissue from patients subjected to LSCC surgical resection at The Second Affiliated Hospital of Harbin Medical University from January 2010 to June 2017 were collected. All the patients were pathologically confirmed and the fresh paired cancerous and adjacent noncancerous tissues were collected and frozen in liquid nitrogen immediately after they were obtained during the surgical operation, and then stored at -80°C to prevent RNA loss. Among them, 3 patients were chosen for profile analysis, and all 85 for quantitative real-time PCR (qRT-PCR) validation. Besides, 85 paraffin samples of these LSCC patients were recruited in the present study, and their paired cancerous and noncancerous tissue blocks were collected. For exosome purification, serum samples were collected from LSCC patients and healthy donors from 2015 to 2017. All patients provided written informed consent in accordance with the Declaration of Helsinki. The study protocol was approved by the Ethics Committee of The Second Affiliated Hospital of Harbin Medical University.

Cell culture and plasmid transfection

Normal human bronchial epithelial cell (NHBEC) line and human laryngeal cancer cell lines TU686, TU177, Hep-2, and LSC-1 were obtained from Bena Culture Collection (Beijing, China). All cell lines were routinely cultured in Dulbecco's modified Eagle's medium (DMEM)/F12 (1:1) medium containing 10% fetal bovine serum (Biological Industries, Nanjing, China), 100 U/ml penicillin (Sigma, St. Louis, MO), and 0.1 mg/ml streptomycin (Sigma) in a humidified atmosphere of 5% CO_2 and 95% air at 37°C. A six-well plate was seeded with 5×10^5 cells and incubated for 24 h. The cells were then transfected with the related genes using Lipofectamine™ 2000 (Thermo Fisher Scientific) according to the manufacturer's instructions.

Expression profile analysis of circRNAs

Three pairs of paired LSCC and normal tissues were used for circRNA microarray. Tissues specimens were obtained during operation and immediately frozen at -80°C until further use. The circRNAs chip (ArrayStar Human circRNAs chip; ArrayStar, Rockville, MD, U.S.A.) containing 5639 probes specific for human circRNAs splicing sites was used. Following hybridization and washing of the samples, five pairs of paired cancerous and adjacent noncancerous tissues were analyzed on the circRNAs chips. Exogenous RNAs developed by the External RNA Controls Consortium (ERCC) were used as controls. circRNAs were enriched by digesting linear RNA with RNase R (Epicentre, Madison,

WI, U.S.A.). Labeled RNAs were scanned using a Agilent Scanner G2505C (Agilent Technologies, Santa Clara, CA, U.S.A.). The circRNA microarray process was performed by KangChen Biotech, Inc. (Shanghai, China).

qRT-PCR

The total RNA was isolated from tissues and cell lines using TRIzol reagent (Invitrogen, CA, U.S.A.), and exosomal RNA was extracted from plasma and culture medium using the exoRNeasy Midi Kit (Qiagen, Valencia, CA, U.S.A.) according to the manufacturer's protocol. For circRNAs, RNase R was used to degrade linear RNA, which have poly (A), and amplified by divergent primer. qRT-PCR analysis on circRNA and mRNA was performed using Prime Script RT reagent Kit (TaKaRa) and SYBR Premix ExTaq II (TaKaRa). GAPDH was used as an endogenous control. TaqMan MicroRNA Reverse Transcription kit and Taqman Universal Master Mix II (Applied Biosystems) were used to detect miR-302b-3p and U6 expression. Relative expression values were normalized and calculated to represent FC in gene expression using relative quantitation as $2^{-\Delta\Delta C}{}_{\mathrm{T}}$.

Cell transfection

Cells were seeded in six-well plates and cultured to 60–70% confluence before transfection. According to the manufacturer's instructions, microRNA (miRNA) mimics, inhibitors (Sangon, China), and siRNA (GeneChem, China) were transiently transfected using Lipofectamine 2000 (Invitrogen) at a final concentration of 50 nM. The corresponding negative controls were transfected simultaneously under the same condition. Lentiviral-circRASSF2-RNAi and the negative control lentiviruses were purchased from GeneChem (Shanghai, China) and transfected according to the manufacturer's protocol.

Cell Counting Kit-8 assay

Cell proliferation was measured by the cell proliferation reagent cell counting kit-8 (CCK-8) (Roche, Basel, Switzerland). After the cells (1×10^3/well) were plating in the 96-well microtiter plates (Corning, NY, U.S.A.), 10 μl CCK-8 regents were added to each well at the time of harvest. Two hours later, the absorbance was recorded at 450 nm to determine the cell viability.

Colony formation assay

One hundred transfected cells were seeded in six-well plates. After 2 weeks of incubation, colonies (>200 cells per colony) were stained with Giemsa. The number of colonies was counted. Each experiment was performed in triplicate.

Cell apoptosis analysis

Detecting apoptosis by flow cytometry An annexin V-allophycocyanin (APC)/4',6-diamidino-2-phenylindole (DAPI) double staining kit (Thermo Fisher Scientific) was used to analyze cellular apoptosis. Cells were seeded in six-well plates (5×10^5 cells/well) and then digested with trypsin (Gibco® trypsin-EDTA, Thermo Fisher Scientific), washed with PBS three times, suspended in 500 μl of binding buffer, and then incubated with 5 μl of FITC–conjugated annexin V and 3 μl of PI for 15 min at room temperature in the dark. The stained cells were detected using the BD FACS Aria II flow cytometer (BD Biosciences, Hercules, CA, U.S.A.).

Cell migration and invasion assay

Cell migration and invasion abilities were measured using the 24-well transwell chambers with 8 μm polycarbonate membrane (Corning, NY, U.S.A.). Filter was first pre-coated with 500 ng/ml matrigel solution for cell migration assay (BD, Franklin Lakes, NY, U.S.A.) and incubated for 4 h at 37°C, then 500 μl of 10% FBS medium was placed in the lower chamber, and 100 μl serum-free medium was placed in the upper chamber. After cells were incubated at 37°C for 14–24 h, cells on the upper membrane surface were scraped off. The cell invasion assay is almost the same to the migration assay and the only difference is that the filter do not need to be precoated with 500 ng/ml matrigel solution. Surfaces were fixed with mixture of methanol and glacial acetic acid at the ratio of 3:1 for 30 min and then dried before they were stained with 15% Giemsa solution for 6–8 h. Then stained cells were observed and counted using an inverted microscope and an average number within five randomly chosen fields was obtained.

Western blot

Cells were lysed for extraction of total protein. After measurement of protein concentration, the protein was separated using 10% sodium dodecyl sulfate/polyacrylamide gel electrophoresis (SDS/PAGE) and transferred on to polyvinylidene difluoride (PVDF) membranes (EMD Millipore, Billerica, MA, U.S.A.). After blocking with 5% non-fat milk,

Bioscience Reports (2019) **133** 1053–1066
https://doi.org/10.1042/CS20190110

the membranes were incubated with primary antibodies: anti-IGF-1R (1:1000, Cell Signaling Technology, Danvers, MA, U.S.A.) and anti-TSG101 (1:1000, Proteintech, Chicago, U.S.A.), anti-HSP70 (1:2000, Proteintech, Chicago, U.S.A.) and anti-GAPDH antibody (1:2000; Cell Signaling Technology). Then the membranes were incubated with horseradish peroxidase–conjugated secondary antibodies. Immunoblot signals were visualized using ECL Plus Kit (GE Healthcare, Fairfield, CT, U.S.A.) according to the manufacturer's instructions.

Bioinformatics analysis

Agilent Feature Extraction software (version 11.0.1.1) was used to analyze acquired array images. Data processing were performed using the R software package. Differentially expressed circRNAs with statistical significance between two groups were identified through Volcano Plot filtering. Differentially expressed circRNAs between two samples were identified through Fold Change filtering. The circRNA/microRNA interaction was predicted with Arraystar's home-made software based on TargetScan and miRanda.

Luciferase reporter assay

The Luciferase assay was performed in 293T cell lines. Cells were seeded into 24-well plates in triplicate. After 24 h, the cells were transfected with pmirGLO-circRASSF2-WT (or pmirGLO-circRASSF2-Mut) or pmirGLO-IGF-1R-Wt (or pmirGLO-IGF-1R-Mut) and miR-302b-3p mimic, or miR-NC using Lipofectamine 3000 (Invitrogen). Luciferase activity was measured in cell lysates 24 h after transfection using a Dual Luciferase Reporter System (Promega, Madison, WI, U.S.A.).

In vivo study

Five-week-old nude mice were raised and randomly divided into two groups. For injection, 1×10^7 LSC1 cells transfected with sh-circRASSF2 or sh-NC were suspended in 110 μl of serum-free RPMI or DMEM, and injected subcutaneously in the flank. Tumor growth was monitored every 2–3 days using a caliper. Tumor volume was calculated using the following formula: $V = \text{length} \times \text{width}^2/2$). Five weeks later, the mice were killed and the xenografts were removed. All experimental procedures took place at the Animal Center of The Second Affiliated Hospital of Harbin Medical University and approved by the Animal Ethics Committee of The Second Affiliated Hospital of Harbin Medical University, and animal experiments were performed following the National Institute of Health Guide for the Care and Use of Laboratory Animals.

Immunohistochemistry

Immunohistochemistry (IHC) analysis was performed under manufacturer's instructions. Briefly, the slides were incubated with primary antibodies overnight at 4°C and then incubated with secondary antibodies at room temperature for 2 h. The expression was evaluated using a composite score obtained by multiplying the values of staining intensities (0, no staining; 1, weak staining; 2, moderate staining; 3, strong staining) and the percentage of positive cells (0, 0%; 1, <10%; 2, 10–50%; 3, >50%).

Exosome isolation

The plasma was collected and centrifuged at 3000×***g*** for 15 min to remove cells and cellular debris. Exosomes were isolated using the Exoquick exosome precipitation solution (System Biosciences).

Transmission electron microscopy

Exosomes were suspended in 100 μl of PBS and were fixed with 5% glutaraldehyde at incubation temperature and then maintained at 4°C until transmission electron microscopy (TEM) analysis. According to the TEM sample preparation procedure, we placed a drop of exosome sample on a carbon-coated copper grid and immersed it in 2% phosphotungstic acid solution (pH 7.0) for 30 s. The preparations were observed with a transmission electron microscope (Tecnai G2 Spirit Bio TWIN, FEI, U.S.A.).

Statistical analysis

All data were presented as mean ± S.E.M. Two-tailed unpaired Student's *t* test was used to analyze the statistical difference between two groups, *P*-value less than 0.05 was considered statistically significant.

Table 1 Association between circRASSF2 and clinicopathological characteristics of LSCC patients

Characteristics	circRASSF2		*P*-value
	Low expression (*n*=32)	High expression (*n*=53)	
Age (years)			
<60	10	23	0.358
≥60	22	30	
Drinking			
Yes	9	25	0.111
No	23	28	
Smoking			
<400 (y×p)	19	24	0.265
≥400 (y×p)	13	29	
T-category			
T1-T2	23	21	0.006
T3-T4	9	32	
Lymph node metastasis			
N0	22	20	0.007
N1 or N2	10	33	
Differentiation			
Well	15	28	0.657
Moderate-to-Poor	17	25	

Results

Expression profiles of circRNAs in human LSCC tissues

To identify LSCC-related circRNAs, we analyzed the expression profile consisting of three pairs of LSCC and normal tissues by using circRNA microarray. As a result, 527 circRNAs were up-regulated, whereas 414 circRNAs were down-regulated based on the log2 (FCs) ≥ 2, $P<0.05$, and FDR < 0.05. The heatmap showed top ten up-regulated and down-regulated circRNAs between LSCC tissues and non-cancerous matched tissues (Figure 1A), which were then subjected to validation by RT-qPCR. There was an increasing trend in hsa_circ_0059354 (chr20: 4760668-4766974) levels from non-cancerous matched tissues to LSCC tissues, with more than four-fold change from microarray analysis. By browsing the human reference genome (GRCh37/hg19), we identified that circ_0059354 is derived from RASSF2, which is located on chromosome 20, and thus we named it circRASSF2. Next, we examined the expression of these 10 mostly changed circRNAs in LSCC and matched non-tumor tissue samples from 30 patients to confirm their expression, and we found that circRASSF2 expression was consistently and significantly increased in LSCC tumor tissues as compared with that in matched controls (Figure 1B; $P<0.001$).

To investigate the clinical significance of circRASSF2 expression in LSCC patients, the expression of circRASSF2 in LSCC tissues was then confirmed in 85 LSCC patients, and the results showed that circRASSF2 expression was significantly increased in 78.82% (67 of 85) LSCC tissues as compared with that in the matched non-tumor tissues (Figure 1C; $P<0.01$). In addition, the up-regulated expression of circRASSF2 was positively associated with metastasis (Figure 1D; $P<0.01$). In addition, we explored the association between circRASSF2 expression and LSCC clinical–pathological characteristics. Correlation regression analysis of 85 samples demonstrated that high expression of circRASSF2 was significantly correlated with advanced T category ($P=0.006$) and poor lymph node metastasis ($P=0.007$) (Table 1).

Moreover, we analyzed head and neck squamous cell carcinoma (HNSCC) dataset including LSCC from the TCGA database (tumor group, 519; normal group, 44;), and found that the level of linear mRNA of RASSF2 was not up-regulated in HNSCC tissues (Figure 1E). However, Kaplan–Meier survival analysis from TCGA HNSCC datasets suggested that high expression of linear mRNA of RASSF2 in HNSCC tissues is significantly associated with disease-free survival (DFS) (log-rank test, $P=0.005$, Figure 1F).

circRASSF2 promotes cell proliferation and migration of LSCC cells *in vitro*

To choose the LSCC cell lines used for silencing or overexpression of, we checked the expression of circRASSF2 in a panel of LSCC cell lines. Compared with normal cell line NHBEC, the abundance of circRASSF2 was significantly

Bioscience Reports (2019) **133** 1053–1066
https://doi.org/10.1042/CS20190110

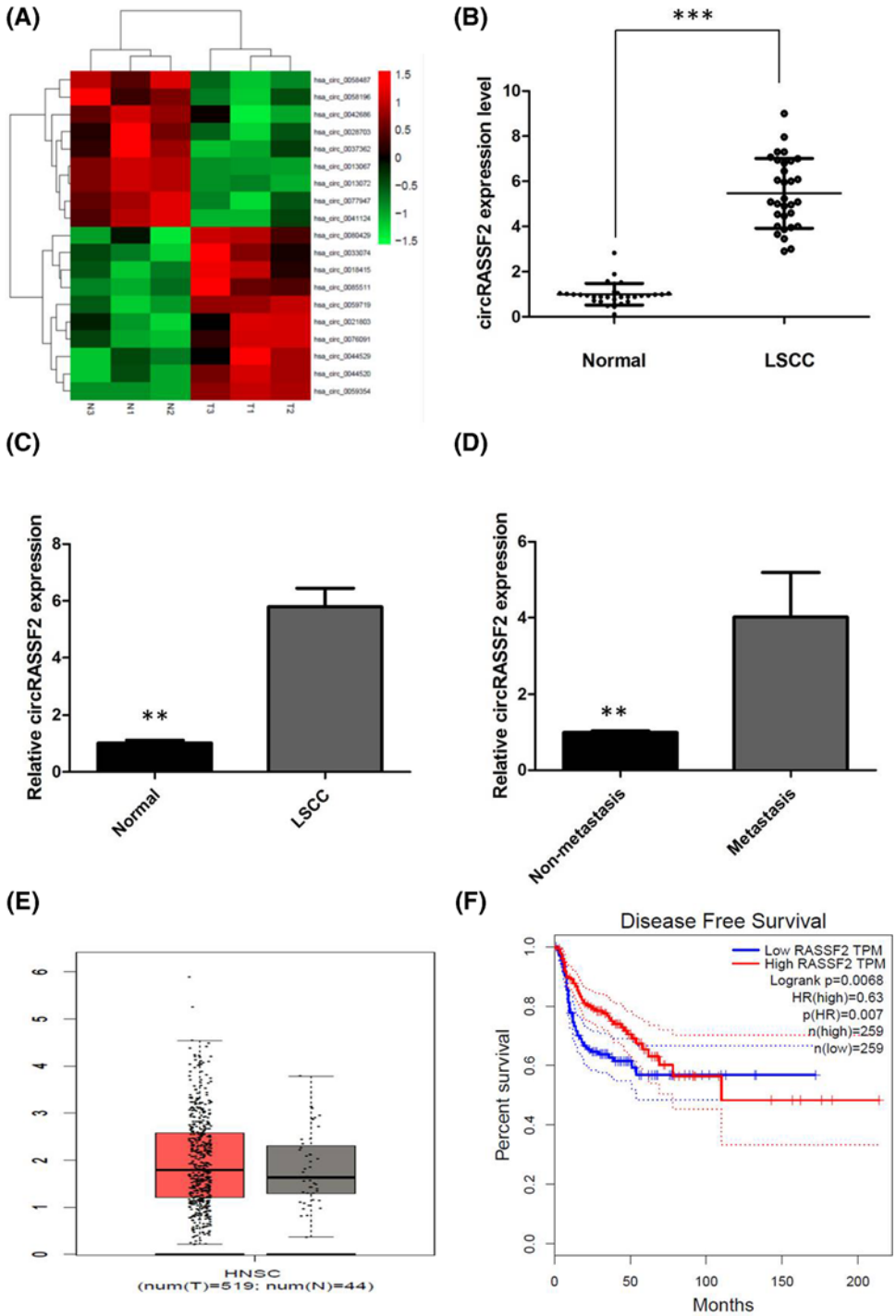

Figure 1. Deregulated circRNAs in LSCC tumor tissues

(**A**) The heatmap showed the top ten most increased and decreased circRNAs in LSCC tissues as compared with that in the matched non-tumor tissues analyzed by circRNAs Arraystar Chip. (**B**) The levels of circRASSF2 was significantly increased in LSCC tumor tissues as compared with that in matched non-tumor tissues of 30 LSCC patients. ***$P<0.001$ (**C**) The differential expression of circRASSF2 in LSCC tissues and matched non-tumor tissues of 85 patients as indicated. **$P<0.01$ (**D**) The levels of circRASSF2 in LSCC patients with metastasis were significantly higher than that in patients without metastasis. **$P<0.01$ (**E**) RASSF2 expression in HNSCC and normal samples from the TCGA HNSCC dataset. (**F**) Kaplan–Meier analyses of the correlations between RASSF2 expression and DFS of 590 patients from the TCGA HNSCC dataset. Log-rank test was used to calculate *P* values. Abbreviation: HNSCC, head and neck squamous cell carcinoma.

increased in various LSCC cell lines, including TU686, TU177, Hep-2, and LSC-1, with LSC1 expressing the highest level of circRASSF2 (Supplementary Figure S1A). Therefore, LSC1 cells were selected for silencing of circRASSF2, and TU686 cells were selected for overexpression of circRASSF2.

Hence, we focused on the functional role of circRASSF2. To investigate whether circRASSF2 is essential for LSCC, we performed a loss-of-function analysis. We knocked down circRASSF2 via specific siRNA targeting the splice junction of circRASSF2. After transfection with circRASSF2 siRNA into LSC1 cells, experimental validation using RT-qPCR showed that depletion of circRASSF2 with siRNA resulted in a clear decrease in the expression of circRASSF2, while *RASSF2* mRNA expression was not affected (Figure 2A; $P<0.001$). In addition, we constructed the circRASSF2 overexpressing plasmid (pCD-circRASSF2) with circular frame and circRASSF2 sequence, and found circRASSF2 could be significantly overexpressed in TU686 cells (Figure 2B; $P<0.001$). CCK-8 assay showed that circRASSF2 knockdown significantly repressed cell proliferation of LSC1 cells at each time point (72 and 96 h; Figure 2C; $P<0.01$). We also found that the colony-forming ability of LSC1 cells was significantly repressed by si-circRASSF2 (Figure 2D and Supplementary Figure S1B; $P<0.01$). Flow cytometric analysis showed that the percentage of apoptotic cells was significantly induced in circRASSF2 siRNA transduced LSC1 cells than control cells (Figure 2E and Supplementary Figure S1C; $P<0.01$). Transwell migration and Matrigel invasion assay showed that circRASSF2 knockdown significantly repressed the ability of cell migration and invasion of LSC1 cells (Figure 2F and Supplementary Figure S1D; $P<0.01$). While circRASSF2 overexpression promoted cell colony-forming ability, and inhibited apoptosis of TU686 cells (Supplementary Figure S1B,C; $P<0.01$).

circRASSF2 serves as a sponge for miR-302b-3p in LSCC

To investigate the potential miRNAs associated with circRASSF2, TargetScan and miRanda database were used, and the most potentially complementary binding miRNAs were presented. Among these target miRNAs, we found that circRASSF2 has a binding site for miR-302b-3p (Figure 3A). Dual-luciferase reporter assay was practiced for the exploration of whether miR-302b-3p functioned a target of circRASSF2. We discovered luciferase activity was remarked decreased with the cell transfection of miR-302b-3p mimics and circRASSF2-wt rather than co-transfection of NC and circRASSF2-wt, meanwhile, cells transfection of miR-302b-3p mimics and circRASSF2-mut had no effects on luciferase activity (Figure 3B; $P<0.01$). We examined the expression of miR-302b-3p by qRT-PCR in LSCC and matched non-tumor tissue samples from 85 patients. The results of qRT-PCR showed lower expression of miR-302b-3p in LSCC tissues than in matched non-tumor tissues (Figure 3C; $P<0.01$). Next, we measured the levels of miR-302b-3p expression in various LSCC cell lines (Figure 3D; $P<0.01$). LSC1 cells showed the lowest expression of miR-302b-3p, and TU686 cells showed higher expression of miR-302b-3p, indicating the opposite result to circRASSF2 expression. Subsequently, the effect of circRASSF2 on miR-302b-3p expression was evaluated in LSC1 cells. However, we could not found obvious regulation of miR-302b-3p level owing to circRASSF2 knockdown or overexpression (Figure 3E).

To investigate the role of miR-302b-3p on LSCC carcinogenesis, miR-302b-3p mimics or inhibitor was transfected into LSCC cell lines and the proliferation curves were performed (Supplementary Figure S2A). CCK-8 assay showed that TU686 cells transfected with miR-302b-3p inhibitor grew at a dramatically higher rate as compared with controls, while miR-302b-3p overexpression markedly inhibits the cell growth of LSC1 cells when compared with cells transfected with miR-nc (Figure 4A,B; $P<0.01$). Our results showed that the proliferation-suppressing effect of si-circRASSF2 was reversed by a miR-302b-3p inhibitor (Figure 2C). Collectively, these data indicate that miR-302b-3p can inhibit LSCC cells proliferation, which inversely correlates with the effects of circRASSF2 in LSCC cells.

IGF-1R is a direct target of miR-302b-3p

TargetScan, PicTar, and miRanda were then applied used to predict target genes for miR-302b-3p, and IGF-1R was one of the best candidates. Comparison of the human sequence with other species revealed that the targeting sequence was highly conserved among different species (Figure 4C). Then, we constructed luciferase reporter assay, the result showed that miR-302b-3p overexpression significantly reduced the luciferase activity of the IGF-1R-wt, but not the IGF-1R-mut in 293T cells which confirmed the targeting relationship between miR-302b-3p and IGF-1R (Figure 4D; $P<0.01$). In addition, we found that increased miR-302b-3p expression dramatically decreased the expression of IGF-1R in LSC1 cells, while transfection of the miR-302b-3p inhibitor increased the expression of IGF-1R in TU686 cells (Figure 4E and Supplementary Figure S2B). We also found that IGF-1R expression was higher in LSCC tissues compared with in their normal counterparts (Supplementary Figure S2C). Taken together, the above data suggest that miR-302b-3p directly regulates oncogene IGF-1R expression in LSCC cells.

Bioscience Reports (2019) **133** 1053–1066
https://doi.org/10.1042/CS20190110

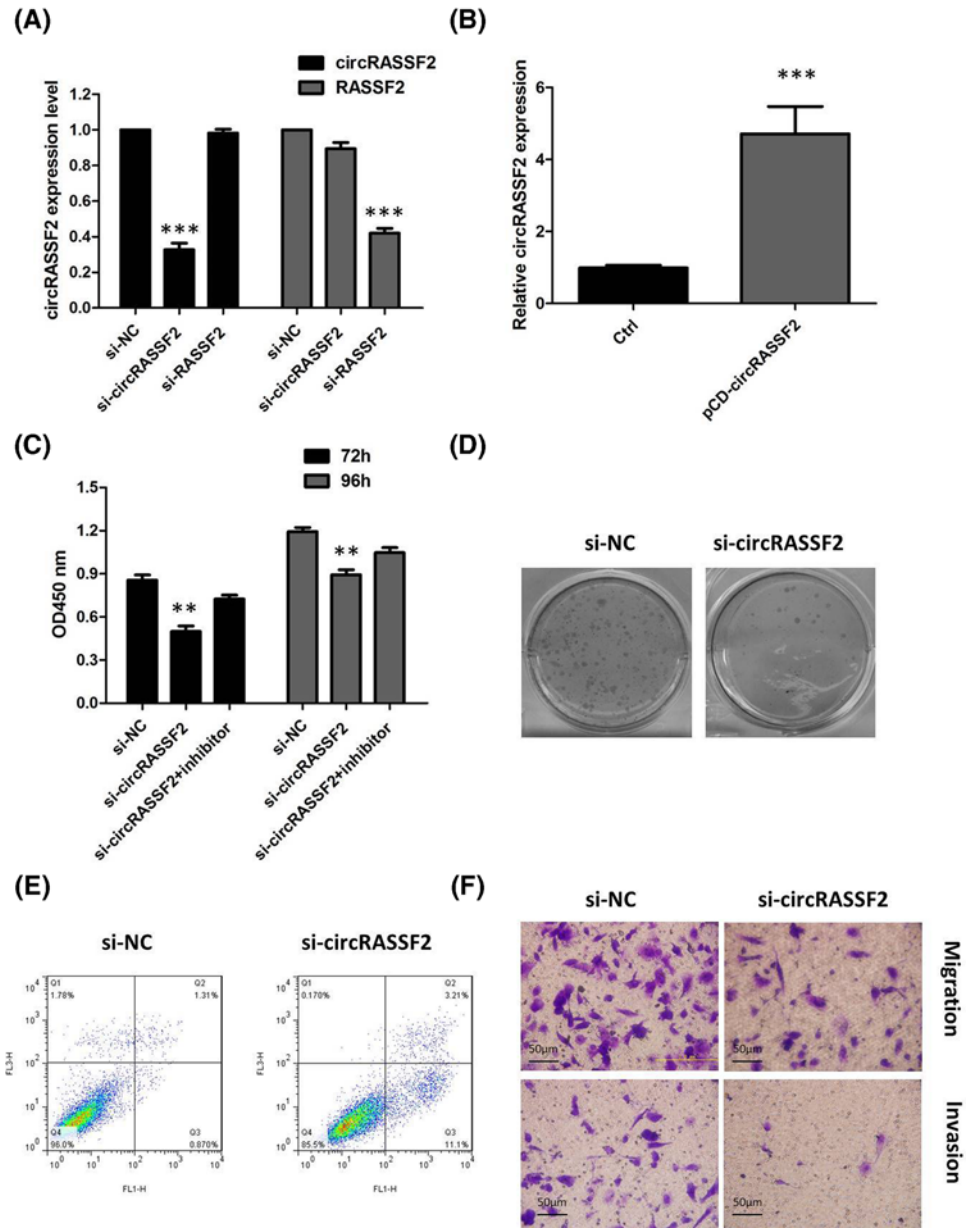

Figure 2. circRASSF2 promotes cell proliferation and migration of LSCC cells *in vitro*

(**A**) RT-qPCR for circRASSF2 and RASSF2 in LSC1 cells treated with si-circRASSF2 or si-RASSF2. Data are the means ± S.D. of three experiments. (**B**) RT-qPCR for circRASSF2 in TU686 cells transfected with control vector or circRASSF2 overexpression plasmid. Data are the means ± S.D. of three experiments. (**C**) CCK-8 assay showed that circRASSF2 knockdown significantly repressed cell proliferation of LSC1 cells, miR-302b-3p inhibitor abolishes the suppression effect of circRASSF2 knockdown. OD values are obtained at 24, 48, 72, and 96 h after transfection. (**D**) Colony formation assay showed that circRASSF2 knockdown significantly reduced cancer cell colony forming ability of LSC1 cells. (**E**) Flow cytometric analysis showed that circRASSF2 knockdown significantly induced apoptosis of LSC1 cells. (**F**) Transwell assay showed that circRASSF2 knockdown significantly inhibited the migration ability of LSC1 cells. Data are the means ± S.D.of three experiments. ***$P<0.001$; **$P<0.01$.

circRASSF2 regulates IGF-1R by sequestering miR-302b-3p

To identify whether circRASSF2 regulates LSCC cell proliferation and IGF-1R expression by inhibiting miR-302b-3p, we performed rescue experiments. There was no notable change in IGF-1R expression when cells were simultaneously treated with a circRASSF2 siRNA and an miR-302b-3p inhibitor (Supplementary Figure S2D), indicating that an

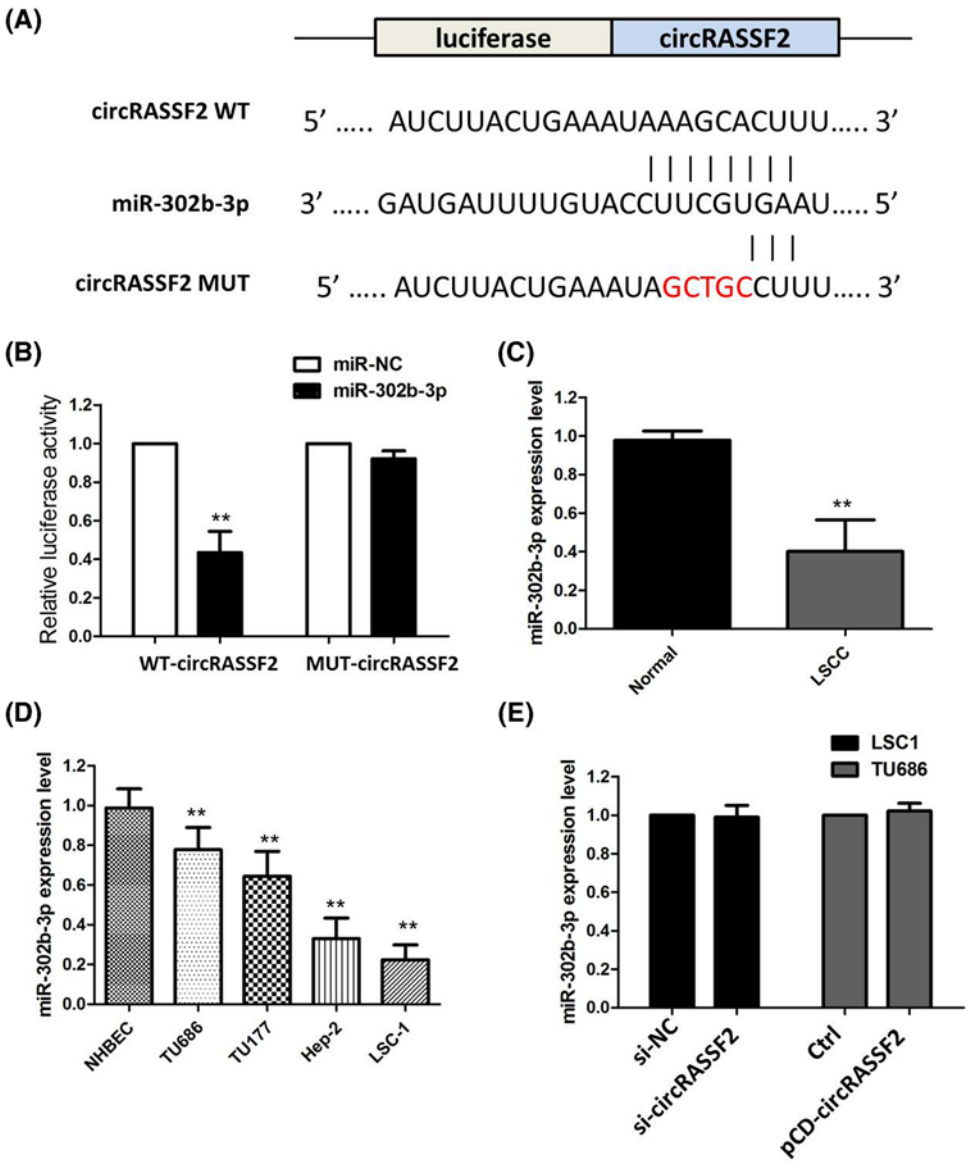

Figure 3. circRASSF2 serves as a sponge for miR-302b-3p in LSCC

(**A**) miRNA response elements (MREs) are shown by which circRASSF2 sequesters miR-302b-3p. Mutations were generated in MREs. (**B**) Dual luciferase reporter show significant reduction in luciferase activity of the wild-type and luciferase activity is restored by the mutant sequence. (**C**) The levels of miR-302b-3p were significantly decreased in LSCC tumor tissues as compared with that in matched non-tumor tissues of 85 LSCC patients. (**D**) The levels of miR-302b-3p in LSCC cells, compared with that in a non-tumorigenic cell, NHBEC. (**E**) The effect of circRASSF2 knockdown or overexpression on miR-302b-3p expression. Data are the means ± S.D. of three experiments. $^{**}P<0.01$.

miR-302b-3p inhibitor could significantly rescue the decrease in IGF-1R induced by silencing circRASSF2. These data suggested that circRASSF2 regulated the LSCC progression via the miR-302b-3p/IGF-1R axis.

Knockdown of circRASSF2 suppressed tumor growth *in vivo*

To determine the effect of circRASSF2 *in vivo*, LSC1 cells stably transfected stable circRASSF2 knockdown (sh-circRASSF2-LSC1) or negative control (sh-NC-LSC1) were injected into the flanks of nude mice. As shown in Figure 5A,B, the results showed that circRASSF2 depletion repressed growth rate and tumor weight of xenograft tumors. In addition, IHC was conducted to determine whether circRASSF2 affects the expression of proliferation marker Ki67 in xenograft tumor tissues ($P<0.01$). IHC assay showed that the tumors treated with

Bioscience Reports (2019) **133** 1053–1066
https://doi.org/10.1042/CS20190110

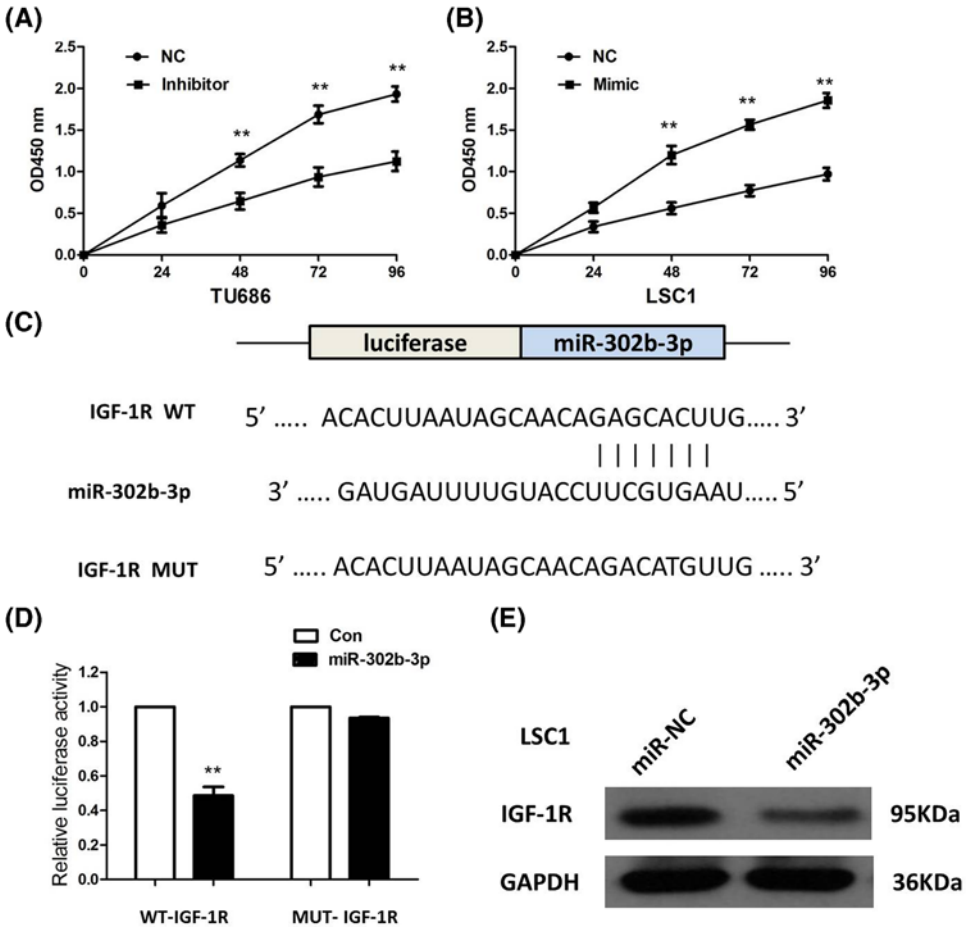

Figure 4. IGF-1R is a direct target of miR-302b-3p

(**A**,**B**) CCK-8 assay showed that TU686 cells transfected with miR-302b-3p inhibitor grew at a dramatically higher rate as compared with controls, while miR-302b-3p overexpression markedly inhibits the cell growth of LSC1 cells when compared with cells transfected with miR-nc. (**C**) MiR-302b-3p is highly conserved across species and binding sites within seed region sequence in the 3′-UTR of human IGF-1R. (**D**) Luciferase assay in HEK293 cells. pmirGLOIGF- 1R-wt or pmirGLO-IGF-1R-mt vector was co–transfected with miR-302b-3p vector. Luciferase activity in pmirGLOIGF-1R-wt group denoted a statistically significant decrease following ectopic expression of miR-302b-3p. (**E**) Overexpression of miR-302b-3p suppressed the expression of IGF-1R in LSCA cells. Data are the means ± S.D. of three experiments. $^{**}P<0.01$.

sh-circRASSF2-LSC1 displayed a decreased proliferation percentage of Ki-67 positive tumor cells compared with sh-NC-LSC1 xenografts (Figure 5C,D; $P<0.01$). Collectively, these results suggested that knockdown of circRASSF2 can suppress LSCC progression *in vivo*.

CircRASSF2 is secreted by exosomes into serum of LSCC patients

Finally, in our current study, we collected abundant serums from 30 LSCC patients and 22 normal people. After isolation of serum exosomes by sequential centrifugation, TEM analysis showed that isolated LSCC-secreted exosomes had similar morphologies (30–150 nm in diameter) and exhibited a round-shaped appearance (Figure 6A). The NTA results demonstrated that isolated LSCC-secreted exosomes showed a similar size distribution, and the peak size range was 80–135 nm. Western blot analysis confirmed the high presence of the exosomal markers TSG101 and HSP70 (Figure 6B). Our results showed that circRASSF2 expression is detectable in extracted serum exosomes derived from LSCC patients (Figure 6C; $P<0.01$). Furthermore, there was a significant inverse correlation between the expression levels of circRASSF2 and miR-302b-3p in serum exosomes derived from LSCC patients (Figure 6D, $r = -0.523$; $P=0.003$).

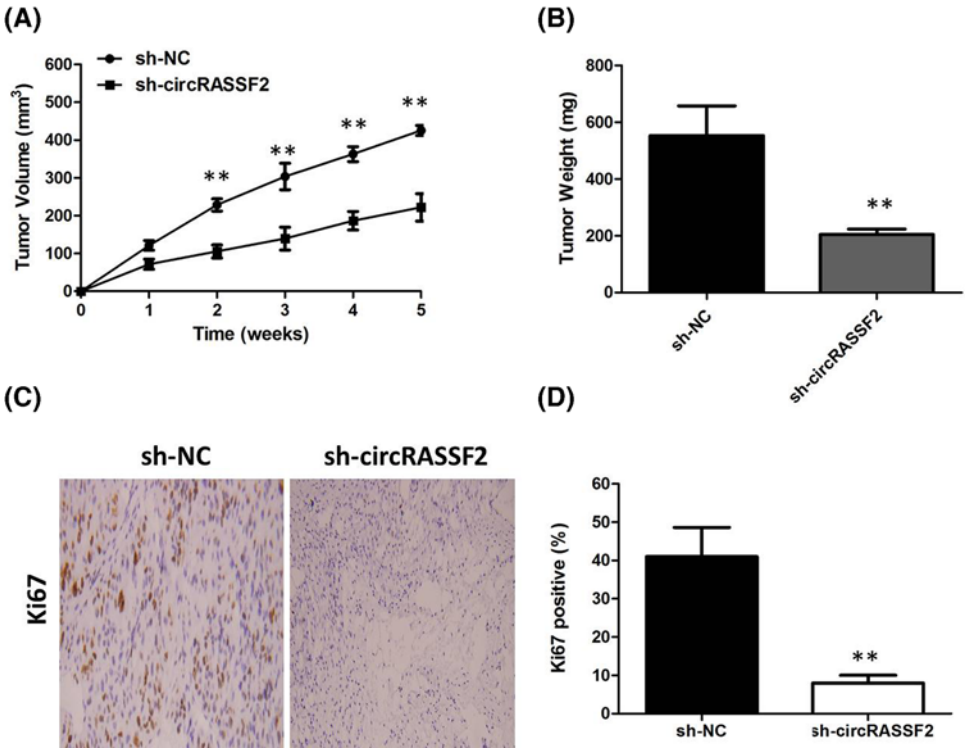

Figure 5. Knockdown of circRASSF2 suppressed tumor growth *in vivo*

(**A**) circRASSF2 knockdown inhibits LSC1 tumor growth *in vivo*. The tumor volume curve of nude mice was analyzed. (**B**) The tumor weights of nude mice were measured. (**C**) IHC analysis were performed to examine the expression levels of proliferation marker Ki-67 in tumors of nude mice. (**D**) F, Knockdown of circRASSF2 significantly decreased the percentage of Ki-67 positive cells in tumors of nude mice compared with that of sh-NC-LSC1 xenografts. $^{**}P<0.01$.

Discussion

The roles of circRNAs in carcinogenesis and cancer progression have attracted much attention, however, the expression and function of circRNAs in LSCC development are still largely elusive. Thus, the purpose of the present study was to identify more circRNAs molecules that may be potentially used in the treatment of LSCC patients through the screening of circRNAs microarray. We analyzed the expression profiles of circRNAs from LSCC and matched non-tumor normal tissues by microarray, and focused on the role and underlying mechanism of the increased circRASSF2 expression in LSCC. In our present study, we identified that circRASSF2 was up-regulated in LSCC and higher expression of circRASSF2 was positively correlated with metastasis of LSCC patients. Our subsequent studies demonstrate that circRASSF2 knockdown decreased cell proliferation and migration, whereas circRASSF2 overexpression had the opposite results. These observations of tumor growth were verified in a mouse xenograft model. Specifically, we also showed mechanistically that circRASSF2 promotes the progression of LSCC by acting as the sponge of miR-302b-3p. Finally, we showed that overexpressed circRASSF2 was secreted by exosomes into the serum of LSCC patients, suggesting that circRASSF2 might be a novel clinical molecular marker for the diagnosis of LSCC patients.

As a novel class of ncRNAs, accumulating evidence suggests that circRNAs may be used as tumor biomarkers and regulators [14]. It has been elucidated that some circRNAs may be potential biomarkers for the diagnosis of various cancers. Zhang et al. [15] found that circLARP4 was down-regulated in gastric cancer tissues and inhibited the proliferation and invasion of gastric cancer cells by sponging miR-42435. Chen et al. [16] showed that circRNA_100290 was up-regulated in oral cancer and functioned as sponge of the miR-29 family. However, the expression and biological function of circRNAs in LSCC are poorly understood. In our study, used a high-throughput microarray platform to evaluate circRNA expression profiles in LSCC patients. We first demonstrated that circRASSF2 was an important circRNA frequently up-regulated in LSCC tissue, contributing to the aggressive clinical LSCC phenotype. Importantly, further functional studies showed that circRASSF2 promoted cell proliferation and migration of LSCC cells.

Bioscience Reports (2019) **133** 1053–1066
https://doi.org/10.1042/CS20190110

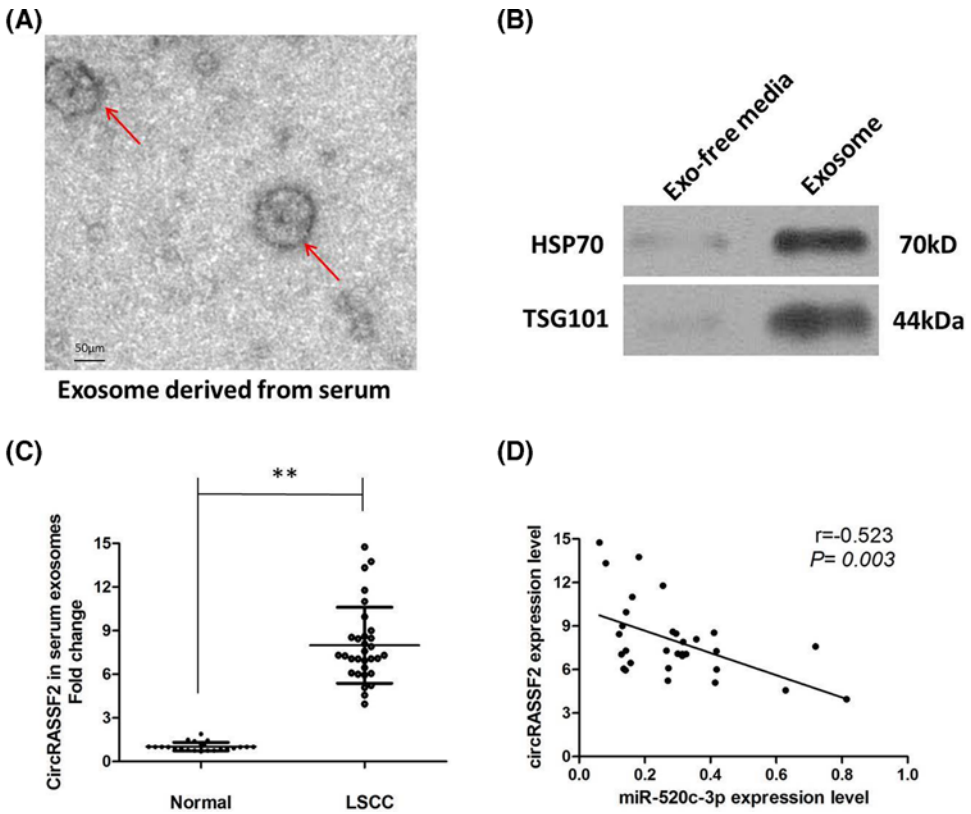

Figure 6. CircRASSF2 is secreted by exosomes into serum of LSCC patients

(**A**) CircRASSF2 was secreted into exosomes derived from serum of LSCC patients. A representative image of exosome (indicated by red arrows) derived from serum of LSCC patients detected from electron microscope. (**B**) WB showing the expression of TSG101 and HSP70, which are the markers of exosome from purified serum exosome. (**C**) RT-qPCR for the abundance of CircRASSF2 in serum exosomes. The levels of CircRASSF2 in serum exosomes from LSCC patients were significantly higher than that in normal individuals; (**D**) the expression levels of CircRASSF2 were negatively correlated with that of miR-302b-3p in the exosomes extracted from serum of LSCC patients. Data are the means ± S.D. of three experiments. $^{**}P<0.01$.

It is well known that competing endogenous RNA (ceRNA) network is an important regulatory model and circRNAs could act as a ceRNA through regulating miRNAs [17]. Based on bioinformatics analysis, it was assumed that the circRASSF2/miR-302b-3p/IGF-1R axis plays a pivotal role in LSCC progression. Bioinformatics analysis and luciferase reporter assay indicated that circRASSF2 could sponge miR-302b-3p, and IGF-1R was the target of miR-302b-3p. Cytological function experiment revealed that circRASSF2 and miR-302b-3p have reverse effects in cell phenotype. A miR-302b-3p inhibitor could rescue biological changes induced by silencing of circRASSF2. Taken together, the study revealed that a circRASSF2/miR-302b-3p/IGF-1R axis exists in LSCC, and that circRASSF2 negatively regulates miR-302b-3p. The aberrantly up-regulated circRASSF2 accompanied with down-regulated miR-302b-3p may be potentially used for early diagnosis and determining prognosis in LSCC patients.

Exosomes are membrane vesicles of an average 30–100 nm diameter, containing miRNA, mRNA, and proteins, and are released by cells into the extracellular microenvironment [18]. Recently, it has been shown that circRNAs can be secreted by serum exosome from cancer cells into circulation, with unknown pathological functions [19]. Here, we performed TEM to reveal the shapes and size of exosomes from plasma of LSCC patients. Notably, we found that the highly expressed circRASSF2 could be examined to serum exosomes of LSCC patients.

Conclusions

In summary, we provided an efficient way to screen for valuable oncofetal molecules associated with LSCC. Our current work revealed that the circRASSF2 was an oncogenic factor that promotes tumorigenesis by

serving as a ceRNA to regulate IGF1R expression by sponging miR-302b-3p. Further understanding of the circRASSF2/miR-302b-3p/IGF-1R axis may provide a novel therapeutic strategy for LSCC in the future.

Clinical perspectives

- The molecular mechanisms of LSCC carcinogenesis are not fully understood, and the roles of circRNAs in LSCC still remain largely uncovered.
- We identified that circRASSF2 was up-regulated in LSCC and higher expression of circRASSF2 was positively correlated with LSCC patients metastasis. Our subsequent studies demonstrate that circRASSF2 knockdown decreased cell proliferation and caused a dramatic decrease in cell colony formation, whereas circRASSF2 overexpression has the opposite results. These observations of tumor growth were verified in a mouse xenograft model. Specifically, we also showed mechanistically that circRASSF2 promotes the progression of LSCC by acted as the sponge of miR-302b-3p. Finally, we showed that overexpressed circRASSF2 was secreted by exosomes into the serum of LSCC patients.
- CircRASSF2 is a central component linking circRNAs to progression of LSCC via a miR-302b-3p/IGF-1R axis.

Funding
This work was supported by the National Science Foundation of China [grant numbers 81572647, 81772874, 81372902]; and the Postdoctoral Scientific Research Developmental Fund [grant number LBH-Q16157].

Author Contribution
Ming Liu performed primers design and experiments. Linli Tian and Jing Cao contributed flow cytometry assay and animal experiments. Hui Jiao and Jiarui Zhang collected and classified the human LSCC tissue samples. Xiuxia Ren and Xinyu Liu contributed to RT-PCR and qRT-PCR. Yanan Sun analyzed the data. Linli Tian and Jing Cao wrote the paper. All authors read and approved the final manuscript.

Ethics approval and consent to participate
The present study was approved the Institutional Review Board of The Second Affiliated Hospital, Harbin Medical University.

Consent for publication
We have received consent from individual patients who have participated in the present study. The consent forms will be provided upon request.

Competing Interests
The authors declare that there are no competing interests associated with the manuscript.

Abbreviations
CCK-8, Cell Counting Kit-8; ceRNA, competing endogenous RNA; circRNA, circular RNA; DMEM, Dulbecco's modified Eagle's medium; FC, fold change; FDR, false discovery rate; HNSCC, head and neck squamous cell carcinoma; IGF-1R, insulin-like growth factor 1 receptor; IHC, immunohistochemistry; LSCC, laryngeal squamous cell carcinoma; miRNA, microRNA; ncRNA, non-coding RNA; NHBEC, normal human bronchial epithelial cell; NTA, nanoparticle tracking analysis; qRT-PCR, quantitative real-time PCR; TCGA, the Cancer Genome Atlas; TEM, transmission electron microscopy.

References
1 Marioni, G., Marchese-Ragona, R., Cartei, G., Marchese, F. and Staffieri, A. (2006) Current opinion in diagnosis and treatment of laryngeal carcinoma. *Cancer Treat. Rev.* **32**, 504–515, https://doi.org/10.1016/j.ctrv.2006.07.002
2 Almadori, G., Bussu, F., Cadoni, G., Galli, J., Paludetti, G. and Maurizi, M. (2005) Molecular markers in laryngeal squamous cell carcinoma: towards an integrated clinicobiological approach. *Eur. J. Cancer* **41**, 683–693, https://doi.org/10.1016/j.ejca.2004.10.031

Bioscience Reports (2019) **133** 1053–1066
https://doi.org/10.1042/CS20190110

3 Calkovsky, V. and Hajtman, A. (2015) Primary prosthetic voice rehabilitation in patients after laryngectomy: applications and pitfalls. *Adv. Exp. Med. Biol.* **852**, 11–16, https://doi.org/10.1007/5584˙2014˙104
4 Ren, J., Zhu, D., Liu, M., Sun, Y. and Tian, L. (2010) Downregulation of miR-21 modulates Ras expression to promote apoptosis and suppress invasion of laryngeal squamous cell carcinoma. *Eur. J. Cancer* **46**, 3409–3416, https://doi.org/10.1016/j.ejca.2010.07.047
5 Ashwal-Fluss, R., Meyer, M., Pamudurti, N.R., Ivanov, A., Bartok, O., Hanan, M. et al. (2014) circRNA biogenesis competes with pre-mRNA splicing. *Mol. Cell* **56**, 55–66, https://doi.org/10.1016/j.molcel.2014.08.019
6 Starke, S., Jost, I., Rossbach, O., Schneider, T., Schreiner, S., Hung, L.H. et al. (2015) Exon circularization requires canonical splice signals. *Cell Rep.* **10**, 103–111, https://doi.org/10.1016/j.celrep.2014.12.002
7 Qu, S., Yang, X., Li, X., Wang, J., Gao, Y., Shang, R. et al. (2015) Circular RNA: a new star of noncoding RNAs. *Cancer Lett.* **365**, 141–148, https://doi.org/10.1016/j.canlet.2015.06.003
8 Memczak, S., Jens, M., Elefsinioti, A., Torti, F., Krueger, J., Rybak, A. et al. (2013) Circular RNAs are a large class of animal RNAs with regulatory potency. *Nature* **495**, 333–338, https://doi.org/10.1038/nature11928
9 Fan, Y., Xia, X., Zhu, Y., Diao, W., Zhu, X., Gao, Z. et al. (2018) Circular RNA expression profile in laryngeal squamous cell carcinoma revealed by microarray. *Cell. Physiol. Biochem.* **50**, 342–352, https://doi.org/10.1159/000494010
10 Xu, R., Greening, D.W., Zhu, H.J., Takahashi, N. and Simpson, R.J. (2016) Extracellular vesicle isolation and characterization: toward clinical application. *J. Clin. Invest.* **126**, 1152–1162, https://doi.org/10.1172/JCI81129
11 Abels, E.R. and Breakefield, X.O. (2016) Introduction to extracellular vesicles: biogenesis, RNA cargo selection, content, release, and uptake. *Cell. Mol. Neurobiol.* **36**, 301–312, https://doi.org/10.1007/s10571-016-0366-z
12 Dai, X., Chen, C., Yang, Q., Xue, J., Chen, X., Sun, B. et al. (2018) Exosomal circRNA_100284 from arsenite-transformed cells, via microRNA-217 regulation of EZH2, is involved in the malignant transformation of human hepatic cells by accelerating the cell cycle and promoting cell proliferation. *Cell Death Dis.* **9**, 454, https://doi.org/10.1038/s41419-018-0485-1
13 Li, Y., Zheng, Q., Bao, C., Li, S., Guo, W., Zhao, J. et al. (2015) Circular RNA is enriched and stable in exosomes: a promising biomarker for cancer diagnosis. *Cell Res.* **25**, 981–984, https://doi.org/10.1038/cr.2015.82
14 Holdt, L.M., Kohlmaier, A. and Teupser, D. (2018) Molecular roles and function of circular RNAs in eukaryotic cells. *Cell. Mol. Life Sci.* **75**, 1071–1098, https://doi.org/10.1007/s00018-017-2688-5
15 Zhang, J., Liu, H., Hou, L., Wang, G., Zhang, R., Huang, Y. et al. (2017) Circular RNA_LARP4 inhibits cell proliferation and invasion of gastric cancer by sponging miR-424-5p and regulating LATS1 expression. *Mol. Cancer* **16**, 151, https://doi.org/10.1186/s12943-017-0719-3
16 Chen, L., Zhang, S., Wu, J., Cui, J., Zhong, L., Zeng, L. et al. (2017) circRNA_100290 plays a role in oral cancer by functioning as a sponge of the miR-29 family. *Oncogene* **36**, 4551–4561, https://doi.org/10.1038/onc.2017.89
17 Hansen, T.B., Jensen, T.I., Clausen, B.H., Bramsen, J.B., Finsen, B., Damgaard, C.K. et al. (2013) Natural RNA circles function as efficient microRNA sponges. *Nature* **495**, 384–388, https://doi.org/10.1038/nature11993
18 Dou, Y., Cha, D.J., Franklin, J.L., Higginbotham, J.N., Jeppesen, D.K., Weaver, A.M. et al. (2016) Circular RNAs are down-regulated in KRAS mutant colon cancer cells and can be transferred to exosomes. *Sci. Rep.* **6**, 37982, https://doi.org/10.1038/srep37982
19 Zhao, Z.J. and Shen, J. (2017) Circular RNA participates in the carcinogenesis and the malignant behavior of cancer. *RNA Biol.* **14**, 514–521, https://doi.org/10.1080/15476286.2015.1122162